Impregnation of Tubular Self-Assemblies into Dextran Hydrogels

ARTICLE *in* LANGMUIR · FEBRUARY 2010

Impact Factor: 4.46 · DOI: 10.1021/la902855e · Source: PubMed

Langmuir Article

pubs.acs.org/Langmuir

Impregnation of Tubular Self-Assemblies into Dextran Hydrogels

Guoming Sun[†,§] and Chih-Chang Chu*[,†,‡]

[†]*Fiber and Polymer Science Program, Department of Fiber Science & Apparel Design, Cornell University, Ithaca, New York 14853-4401, and* [‡]*Department of Biomedical Engineering, Cornell University, Ithaca, New York 14853-5201.* [§]*Present address: Department of Chemical and Biomolecular Engineering, Johns Hopkins University, 3400 N Charles St., Baltimore, MD 21218.*

Received August 4, 2009. Revised Manuscript Received September 28, 2009

Amine groups are the building units of proteins. The incorporation of amine groups into polyethylene glycol diacrylate (PEGDA) hydrogel through dextran−allyl isocyanate−ethylamine (Dex-AE) enhances sustained protein release by introducing effective interactions. To investigate such an interaction effect and to improve protein release, we impregnated self-assembled tubular structures from dextran−bromoethylamine (Dex-BH) and dextran−chloroacetic acid (Dex-CA) into Dex-AE/PEGDA hydrogel. The morphology data obtained from scanning electron microscopy (SEM) reveal that pure PEGDA hydrogel had no effect on the distribution of the self-assembled tubules; the introduction of Dex-AE brought about the dispersion of these tubules, and an increase in Dex-AE content led to more evenly distributed structures. Moreover, the implantation of the self-assembled tubules had no distinct effect on the swelling capacity of the hybrid self-assembly embedded hydrogels. The *in vitro* albumin release study was carried out in a pH 7.4 buffer solution; the results show that the implantation of the self-assembly into the hydrogels reduced the burst release and prolonged the protein release time. These findings demonstrate that the impregnation of tubular self-assembly into hydrogel makes the hybrid hydrogel an excellent protein delivery system.

Introduction

Proteins have long been used as therapeutics to treat various diseases (e.g., cancers). Protein therapeutics has grown rapidly in recent years, with a wide range of new protein-based drugs that have been approved by the FDA and are now commercially available.[1] However, therapeutic proteins are fragile to their environment, suffering from instability *in vivo* and short circulating half time. Intelligent drug delivery systems (DDS) that can maintain the bioactivity and prolong release are very desirable.[2] The increased use and continued development of protein therapeutics has thus led to the rapid development of new drug delivery systems.

Polymeric drug deliveries, such as gels, films, micro- and nanospheres, have been extensively studied as protein drug carriers. Hydrogels are three-dimensional polymeric networks that can swell dramatically in the presence of biological fluids while maintaining their structures. They have proven effective for controlled protein release.[2−6] Most hydrogels are more than a drug encapsulating matrix; they also protect proteins from the physiological environment and thus improve their stability *in vivo*. Furthermore, hydrogels have good compatibility with proteins,[7,8] which makes them even more suitable for protein drug delivery. Due to their structural similarity to natural living tissues,[9] hydrogels have found many applications in biomedical fields, such as cell culture and tissue engineering.[10−13] Particular attention has been given to intelligent hydrogels, due to their ability to respond to external stimuli, such as temperature,[14−17] pH,[15,18] electric fields,[19,20] light[21] and glucose.[22]

Hydrogels can be broadly divided into chemically cross-linked and physically cross-linked hydrogels.[23] Physically cross-linked hydrogels,[24−27] including recently emerging self-assembled

*To whom correspondence should be addressed. Telephone: 1-607-255-1938. Fax: 1-607-255-1093. E-mail: cc62@cornell.edu.

(1) Van Tomme, S. R.; Hennink, W. E. *Expert Rev. Med. Devices* **2007**, *4*, 147−164.
(2) Sun, G. M.; Chu, C. C. *Carbohydr. Polym.* **2006**, *65*, 273−287.
(3) Zhang, Y. L.; Chu, C. C. *J. Biomed. Mater. Res.* **2002**, *59*, 318−328.
(4) Zhang, Y. L.; Chu, C. C. *J. Mater. Sci.-Mater. Med.* **2002**, *13*, 667−676.
(5) Van Tomme, S. R.; van Steenbergen, M. J.; De Smedt, S. C.; van Nostrum, C. F.; Hennink, W. E. *Biomaterials* **2005**, *26*, 2129−2135.
(6) Zhang, X. Z.; Wu, D. Q.; Chu, C. C. *Biomaterials* **2004**, *25*, 3793−3805.
(7) Chen, J.; Jo, S.; Park, K. *Carbohydr. Polym.* **1995**, 69−76.
(8) Molina, I.; Li, S. M.; Martinez, M. B.; Vert, M. *Biomaterials* **2001**, *22*, 363−369.
(9) Ratner, B. D.; Hoffman, A. S. Synthetic hydrogels for biomedical applications. *ACS Symp. Ser.* **1976**, 1−36.
(10) Draye, J. P.; Delaey, B.; Van de Voorde, A.; Van Den Bulcke, A.; De Reu, B.; Schacht, E. *Biomaterials* **1998**, *19*, 1677−1687.
(11) De Groot, C. J.; Van Luyn, M. J. A.; Van Dijk-Wolthuis, W. N. E.; Cadee, J. A.; Plantinga, J. A.; Den Otter, W.; Hennink, W. E. *Biomaterials* **2001**, *22*, 1197−1203.
(12) Levesque, S. G.; Lim, R. M.; Shoichet, M. S. *Biomaterials* **2005**, *26*, 7436−7446.
(13) Leach, J. B.; Bivens, K. A.; Patrick, C. W.; Schmidt, C. E. *Biotechnol. Bioeng.* **2003**, *82*, 578−589.
(14) Hoffman, A. S. *J. Controlled Release* **1987**, *6*, 297−305.
(15) Peppas, N. A.; Klier, J., Controlled release by using poly(methacrylic acid-g-ethylene glycol) hydrogels. *J. Controlled Release* **1991**, *16*, 203−214.
(16) Zhang, X. Z.; Sun, G. M.; Wu, D. Q.; Chu, C. C. *J. Mater. Sci.-Mater. Med.* **2004**, *15*, 865−875.
(17) Zhang, X. Z.; Sun, G. M.; Chu, C. C. *Eur. Polym. J.* **2004**, *40*, 2251−2257.
(18) Zhang, X. Z.; Wu, D. Q.; Chu, C. C. *Biomaterials* **2004**, *25*, 4719−4730.
(19) Liu, Z. S.; Calvert, P. *Adv. Mater.* **2000**, *12*, 288−291.
(20) Kim, S. J.; Yoon, S. G.; Lee, Y. M.; Kim, S. I. *Sens. Actuator B-Chem.* **2003**, *88*, 286−291.
(21) Mamada, A.; Tanaka, T.; Kungwatchakun, D.; Irie, M. *Macromolecules* **1990**, *23*, 1517−1519.
(22) Nakamae, K.; Miyata, T.; Jikihara, A.; Hoffman, A. S. *J. Biomater. Sci.—Polym. Ed.* **1994**, *6*, 79−90.
(23) Hennink, W. E.; van Nostrum, C. F. *Adv. Drug Delivery Rev.* **2002**, *54*, 13−36.
(24) Sun, G. M.; Zhang, X. Z.; Chu, C. C. *J. Mater. Sci.—Mater. Med.* **2007**, *18*, 1563−1577.
(25) Inoue, T.; Chen, G. H.; Hoffman, A. S.; Nakamae, K. *J. Bioact. Compat. Polym.* **1998**, *13*, 50−64.
(26) Jeong, B.; Kim, S. W.; Bae, Y. H. *Adv. Drug Delivery Rev.* **2002**, *54*, 37−51.
(27) Boucard, N.; Viton, C.; Domard, A. *Biomacromolecules* **2005**, *6*, 3227−3237.

supramolecular hydrogels,[5,28−30] have shown promising applications in biomedical fields. However, using chemical cross-linking for the design of biodegradable hydrogels continues to be more desirable because of their relatively easy formulation via the control of experimental parameters like type and concentration of cross-linking agents, initiator concentrations, ratio and concentration of precursors.

Dextran is a colloidal, hydrophilic, biocompatible, and nontoxic biodegradable polysaccharide. Structurally, dextran has chemically active hydroxyl groups (i.e., −OH) that can be chemically modified to form hydrogels via cross-linking. Because of these properties, dextran and their hybrids have been extensively investigated as drug and/or gene carriers. For example, dextran-based biomaterials have been employed in cell immobilization[31] and gene transfection[32] and as carriers for a variety of pharmaceutically active drugs.[33−38] In our group, dextran has been intensively investigated as drug carriers, either incorporated with drugs[37] or derived and formulated into various hydrogels.[2−4,16−18,33,38]

In our prior studies,[2,39] we reported hydrogel synthesis from dextran−allyl isocyanate−ethylamine (Dex-AE) and polyethylene glycol−diacrylate (PEGDA). We also examined the effect of precursor factors on hydrogel formation and their *in vitro* release of bovine serum albumin (BSA) and ovalbumine (OVA). These studies revealed that the introduction of amine group to dextran increases protein absorption ability; and both the protein loading and release data indicated that Dex-AE/PEGDA hydrogels improved protein loading and sustained release capability more effectively than pure PEGDA hydrogel; this ability increased as the Dex-AE composition increased. The study on the effect of the degree of substitution of amine groups further confirmed that proteins have such an interaction with amine groups.

In this study, to further examine the effect of amine groups (Dex-AE) on hydrogel property and to improve protein-based drug release, we impregnated the oppositely charged self-assembly system into these hydrogels. We find that dextran-2-bromoethylamine hydrobromine (Dex-BH) and dextran−chloroacetic acid (Dex-CA) can self-assemble into tubular structures in aqueous solution.[40] However, in a previous study, self-assembling tubules tend to stick together during either growth or drying process, and we cannot separate them from each other once they are dried. The tubular self-assembly within the hydrogels will separate tubules from each other in an undisturbed environment. In addition, as amine groups can become protonated and thus charged, it could influence the self-assembly of Dex-BH and Dex-CA. The morphology of the self-assembly impregnated hybrid hydrogels and the effects of concentration of Dex-BH and Dex-CA, the Dex-AE/PEGDA ratio were examined. The swelling property and protein release profiles of these hybrid hydrogels were studied. Ovalbumin (OVA) was chosen as the model protein for the controlled release study.

Scheme 1. Chemical Structure of Dextran Derivatives

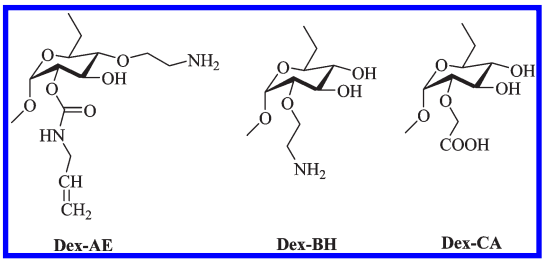

Materials and Methods

Materials. Dextran (MW 6,000 and MW 43,000), allyl isocyanate (AI) and chicken egg albumin (OVA, MW 44287) were purchased from Sigma Chemical Company (St. Louis, MO). Dextran was dried in a vacuum oven for 24 h at 50 °C before use. Dimethyl sulfoxide (DMSO), dibutyltin dilaurate (DBTDL), triethylamine, acryloyl chloride, polyethylene glycol (PEG, MW 4000), triethylamine, 2-Bromoethylamine hydrobromide (BEAHB) and chloroacetic acid (CA) were purchased from Aldrich Chemical Co. (Milwaukee, WI). PEG, BEAHB, and CA were dried in a vacuum oven for 24 h at room temperature before use. Isopropanol was purchased from J.T. Baker (Philipsburg, NJ). The pH 4.0 buffer solution and calcium chloride were purchased from Fisher Chemical (Fair Lawn, NJ). 2-Hydroxy-1-[4-(hydroxyethoxy)-phenyl]-2-methyl-1-propanone (HHPMP) was donated by Ciba Specialty Chemicals Corporation.

Synthesis of Dextran−Allyl Isocyanate−Ethylamine (Dex-AE). Dex-AE was synthesized according to the reported procedure.[2] As illustrated in Scheme 1, the procedure involved the incorporation of allyl isocyanate (Dex-AI) followed by ethylamine (Dex-AE). Briefly, dextran (e.g., 2 g) was first dissolved in anhydrous DMSO (24.0 mL) under dry nitrogen gas at room temperature. DBTDL (0.73 mL) was injected into the solution, and then AI (1.09 mL) was added dropwise. The reaction mixture was stirred for 6 h at room temperature. The resulting polymer (Dex-AI, degree of substitution DS 0.25) was obtained by precipitating in cold excess isopropanol. Dex-AI was further purified by dissolution and precipitation in DMSO and isopropanol, respectively. Dex-AE was synthesized from Dex-AI so that free amine groups could be introduced.

Dried Dex-AI (2.0 g) was first dissolved in anhydrous DMSO (20.0 mL) under nitrogen gas at 50 °C. Triethylamine (11.2 mL) was injected into the above solution. BEAHB (7.5 g) was dissolved in DMSO (10.0 mL) and then added to the above solution dropwise. This reaction solution was stirred for 6 h at 50 °C. The reaction mixture was then cooled to room temperature and filtered by glass Buchner funnel to remove the precipitated Et_3NHBr. The resulting Dex-AE polymer was obtained by precipitating the filtered solution into excess cold isopropyl alcohol. The product was further purified at least 3 times by dissolution and precipitation with DMSO and cold isopropyl alcohol, respectively. The final product was dried at room temperature under vacuum overnight before further use.

Synthesis of Polyethylene Glycol−Diacrylate (PEGDA). According to the published procedures,[2,41] PEG reacted with acryloyl chloride in the presence of triethylamine as a catalyst. At 40 °C, dry PEG (12 g) was dissolved in anhydrous benzene (150.0 mL) under nitrogen atmosphere. Triethylamine (1.78 mL)

(28) Ikada, Y.; Jamshidi, K.; Tsuji, H.; Hyon, S. H. *Macromolecules* **1987**, *20*, 904−906.
(29) de Jong, S. J.; De Smedt, S. C.; Wahls, M. W. C.; Demeester, J.; Kettenes-van den Bosch, J. J.; Hennink, W. E. *Macromolecules* **2000**, *33*, 3680−3686.
(30) Li, J.; Li, X.; Ni, X.; Wang, X.; Li, H.; Leong, K. W. *Biomaterials* **2006**, *27*, 4132−4140.
(31) Massia, S. P.; Stark, J.; Letbetter, D. S. *Biomaterials* **2000**, *21*, 2253−2261.
(32) Azzam, T.; Eliyahu, H.; Makovitzki, A.; Domb, A. J. *Macromol. Symp.* **2003**, 247−261.
(33) Kim, S. H.; Chu, C. C. *J. Biomater. Appl.* **2000**, *15*, 23−46.
(34) Won, C.-Y.; Chu, C.-C. *Carbohydr. Polym.* **1998**, *36*, 327−334.
(35) Kim, I. S.; Jeong, Y. I.; Kim, D. H.; Lee, K. H.; Kim, S. H. *Arch. Pharm. Res.* **2001**, *24*, 69−73.
(36) Chu, C. C. Biodegradable Hydrogels as Drug Controlled Release Vehicles. In *Biomaterials Handbook−Adanced Applications of Basic Sciences and Bioengineering*; Wise, D. L., Ed.; Marcel Dekker Inc.: New York, 2003; pp 871−909.
(37) Won, C. Y.; Chu, C. C., Polysaccharides as Drug Carriers. In *Biomaterials and Bioengineering Handbook*; Wise, D. L., Ed.; Marcel Dekker: New York, 2000; pp 356−371.
(38) Zhang, Y.; Chu, C.-C. *J. Biomater. Appl.* **2002**, *16*, 305−325.
(39) Sun, G.; Zhang, X. Z.; Chu, C. C. *J. Mater. Sci.—Mater. Med.* **2008**, *19*, 2865−2872.
(40) Sun, G. M.; Chu, C. C. *ACS Nano* **2009**, *3*, 1176−1182.
(41) Wu, D. Q.; Zhang, X. Z.; Chu, C. C. *J. Biomater. Sci.—Polym. Ed.* **2003**, *14*, 777−802.

Table 1. Feed Ratio and Composition of the Tubule-Embedded Dex-AE/PEGDA Hydrogel

	Sample ID[a]						
	DBC-0P	DBC-5P	DBC-0	DBC-5	DBC-10	DBC-15	DBC-15′′
Dex-BH (g)	0	0.005	0	0.005	0.010	0.015	0.015
Dex-CA (g)	0	0.005	0	0.005	0.010	0.015	0.015
Dex-AE (g)	0	0	0.045	0.045	0.045	0.045	0.090
PEGDA	0.105	0.105	0.105	0.105	0.105	0.105	0.105
buffer solution[b](mL)	1.0	1.0	1.0	1.0	1.0	1.0	1.0
irgacure 2959 (g)	0.002	0.002	0.002	0.002	0.002	0.002	0.002

[a] All reactions were carried out for 16 h at room temperature. [b] Buffer solution, pH4.0.

and acryloyl chloride (1.22 mL) were subsequently added at 40 °C. The reaction mixture was then heated up to 80 °C and stirred for 3 h. The resulting polymer was precipitated in hexane. It was further purified three times by dissolution and precipitation with benzene and hexane, respectively. The resulting PEGDA was dried overnight in a vacuum oven at room temperature before further use.

Synthesis of Dextran Macromers for Tubular Self-Assembly. The synthesis of dextran−2-bromoethylamine hydrobromide (Dex-BH) and dextran−chloroacetic acid (Dex-AC) were prepared according to our previous method,[40] and their structures are illustrated in Scheme 1. To incorporate amine and carboxylic acid groups, dextran reacted with BEAHB and chloroacetic acid in the presence of triethylamine. An example of Dex-BH synthesis is given here. Predried dextran (2.0 g) was first dissolved at room temperature in anhydrous DMSO (20.0 mL) under nitrogen gas. After 30 min, the solution became clear, and triethylamine (11.2 mL) was injected into the above solution. Meanwhile, BEAHB (7.5 g) was dissolved in DMSO (10.0 mL) and subsequently added to the above solution. This solution was then stirred for 5 h at 50 °C. Dex-BH was then obtained by precipitating the filtered solution into excess cold isopropyl alcohol. The product was further purified at least 3 times by dissolution and precipitation with DMSO and cold isopropyl alcohol, respectively. The final product was dried at room temperature under vacuum overnight before further use. Dex-CA was synthesized using a similar procedure.

Hydrogel Preparation. The Dex-AE/PEGDA hydrogels were prepared via UV-photo-cross-linking. A prior study found that the tube only self-assembled at pH 4.0;[40] therefore, all gels in this study, including pure hydrogel and tube-embedded hydrogels, were formed in a pH 4.0 buffer solution. Meanwhile, our prior study showed that only those Dex-AE to PEGDA precursors' feed ratios ranged from 0/100 to 70/30 led to solid gel form, while the 100/0 feed ratio resulted in a fluid-like gel.[2] Therefore, in this study, we chose 30/70 Dex-AE/PEGDA precursors' feed ratio. The water-soluble initiator Irgacure 2959 was first dissolved in buffer solution. Dex-AE and PEGDA at the feed ratio of 30/70 (weight/weight) were dissolved in 1.0 mL of the above initiator solution. The solution was then irradiated with a long wavelength UV lamp (365 nm, 16 W) for 16 h. The resulting hydrogels were washed in distilled water for 48 h to remove unreacted precursors before further use.

The impregnation of the self-assembling tubes within the hydrogel was prepared similarly. Irgacure 2959 was first dissolved in buffer solution. Dex-BH and Dex-CA were then dissolved in the above initiator solution at the concentration of 2.5 mg/mL, respectively. Then, they were mixed and sonicated for 2 min in a sonicating water bath (Branson 3510R-DTH sonicator, Branson, Danbury, CT). Dex-AE and PEGDA precursors at the feed ratio of 30/70 (weight/weight) were then dissolved into the above solution. The solutions were first stored for at least 2 h for tube self-assembly and then irradiated with the same UV lamp for 16 h. The composition of the self-assembly impregnated hydrogels was expressed as DBC-#(P), where DBC refers to Dex, -BH, and CA respectively, and # refers to the amount of Dex-BH or Dex-CA in mg; where P was only added to those hydrogels made from pure PEGDA. The feed ratio and composition of the self-assembly embedded hydrogels are summarized in Table 1.

Swelling Measurement. The swelling property of the tube-embedded and control hydrogels was gravimetrically determined. Dried hydrogel specimens of known weight (W_d) were immersed in deionized water at room temperature. The swollen hydrogels were removed from water at predetermined intervals and weighed (W_t) after wiping off excess water on the surface with wet filter paper. The swelling ratio was calculated using the following equation:

$$\text{swelling ratio } (\%) = [(W_t - W_d)/W_d] \times 100$$

The hydrogel was considered to reach an equilibrium swelling state when there was no further increase in swelling ratio between two adjacent tests. This test took up to 24 h.

Morphological Study. The morphology of the swollen Dex-AE/PEGDA and the tube-embedded hydrogels was evaluated by scanning electron microscope (SEM, Leica Cambridge Stereoscan 440, Cambridge, UK). The hydrogel specimens were first immersed in distilled water for 24 h. The swollen hydrogels were taken out of water and put immediately in liquid nitrogen. The frozen specimens were then removed from liquid nitrogen and freeze-dried in a Virtis Freeze Drier (Gardiner, NY) for 3 days at −50 °C under vacuum prior to morphological observation. The freeze-dried hydrogels were carefully fractured to reveal the interior structure. The specimens were mounted onto aluminum SEM stubs with double-sided carbon tape and gold sputter-coated (JFC-1200 Fine Coater, Japan) for 40 s. The SEM examination was operated at 25 kV and 12 nA.

Drug Loading and In Vitro Release. *Drug Loading Efficiency into Dex-AE/PEGDA and its Tube-Embedded Hydrogel.* In this study, OVA was chosen as the model drug and preloaded into the Dex-AE/PEGDA as well as the tube-embedded hydrogels. First, 6 mg of OVA was dissolved in the 1.0 mL Irgacure 2959 solution prepared beforehand. Dex-AE and PEGDA at a feed ratio of 30/70 (weight/weight) with a total weight of 0.15 g were then added to the OVA solution and dissolved at room temperature. The solution was irradiated with a long wavelength UV lamp (365 nm, 16 W) for 16 h.

The OVA loading into the tubule-embedded hydrogel is similar to the above method. First, 6 mg of OVA was dissolved in 1.0 mL of initiator solution. Equal amounts of Dex-BH and Dex-CA (e.g., 2.5 mg) were added successively to the OVA solution. Then, they were mixed and sonicated for 2 min in a sonicating water bath (Branson 3510R-DTH sonicator, Branson, Danbury, CT). Dex-AE and PEGDA at a feed ratio of 30/70 (w/w) were then added into the above solution and dissolved at room temperature. The solutions were stored for 2 h and then irradiated with the same UV lamp for 16 h.

The resulting hydrogels, including pure and tube-embedded ones, were taken carefully out of the glass vial and dried in a vacuum oven at room temperature for 3 days before the drug release test. The glass vial was washed with PBS (pH 7.4), and the solution was collected; the amount of OVA in the solution (i.e., unloaded OVA) was determined. The difference between the initial loading amount and unloaded amount was considered as the actual OVA loading quantity in the hydrogels.

Drug Loading Efficiency into the Self-Assembled Tubes. The OVA loading efficiency of the self-assembly was roughly

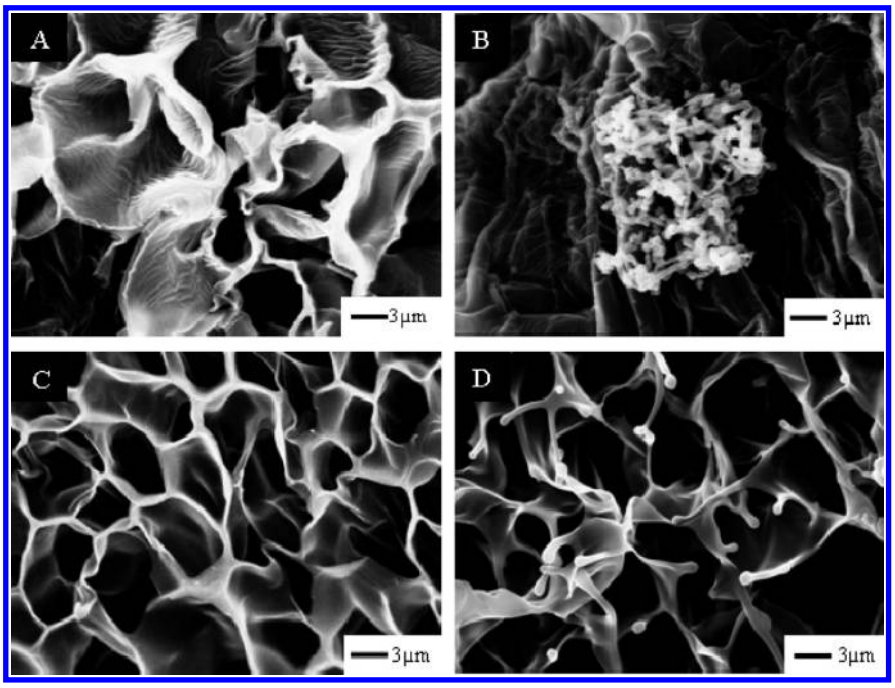

Figure 1. SEM micrographs of the self-assembling embedded hybrid hydrogels: (A) (DBC-0P); (B) (DBC-5P); (C) (DBC-0); (D) (DBC-5).

estimated by loading the same amount of OVA into the same amount of self-assembly without hydrogel precursors. The solution was centrifuged, and the supernatant solution was collected. The difference between the initial loading amount and the unloaded residue of the supernatant solution was defined as the actual OVA loading amount in the self-assembly. The difference between actual OVA loading amount of the tube-embedded hydrogel and the actual loading amount into the self-assembled tubes was defined as the actual OVA loading amount in the hydrogel domain.

Drug Loading Efficiency Determination. The QuantiPro bicinchoninic acid (QP-BCA) protein assay kit was used to determine the OVA loading amount in the hydrogels and the cumulative OVA release over time. The BCA assay solution was prepared according to the manufacturer's instructions. Each OVA-containing hydrogel was immersed in 20.0 mL PBS (pH 7.4) at 37 °C. At predetermined intervals, 1.0 mL of the PBS solution was taken out and transferred to a capped glass vial, and 1.0 mL of blank PBS solution was added back to the immersion solution to maintain the total solution volume. Next, 1.0 mL of QP-BCA assay solution was added to the capped glass vial and incubated at 60 °C for 1 h. The samples were then transferred to a quartz cuvette, and the OVA concentrations in PBS medium at each interval were monitored by the absorption of the medium at $\lambda = 560$ nm on a Perkin−Elmer Lambda 2 UV/vis spectrometer (Norwalk, CT). The concentration of OVA released at a particular interval was calculated from an OVA standard calibration curve. All release studies were carried out in triplicate. The results were presented in terms of cumulative release as a function of time:

$$\text{cumulative release } (\%) = (\sum_{t=0}^{t=t} M_t/M_0) \times 100$$

where $\sum_{t=0}^{t=t} M_t$ is the cumulative amount of released OVA from the hydrogel at time t, and M_0 is the initial amount of loaded OVA in the hydrogel.

To investigate if the OVA loaded in the self-assemblies contributed to the above release, we further choose the same self-assemblies as implanted within DBC-10 (without hydrogel) and loaded with three different amount of OVA, i.e., 2.5%, 5.0%, and 10.0% (w/w) of self-assemblies. The composition of the OVA loaded self-assemblies was expressed as SA10−25, SA10−50, and SA10−100, respectively. The release was carried out same as the loading efficiency test and the result was presented as stated above.

Results and Discussion

Effect of Dex-AE on Self-Assembling Morphology within the Hydrogel. To examine self-assembly morphology under less disturbed conditions and to test the hypothesis that the self-assembly would interact with the hydrogel, two groups of hydrogels were prepared and examined; and their morphologies are shown in Figure 1. The first group is the pure PEGDA hydrogel (Figure 1A) and the self-assembly embedded PEGDA hydrogel (Figure 1B). It is clear that there were no aggregates in the pure PEGDA hydrogel (DBC-0P, Figure 1A), but some aggregates were present in the hydrogel after self-assembly was introduced (DBC-5P, Figure 1B); these aggregates are stuck together. Because the pure hydrogel did not show such aggregates, these aggregates were attributed to the introduction of the self-assembly.

In the second group, Dex-AE was introduced to the hydrogels, and the pure Dex-AE/PEGDA hydrogel (Figure 1C) and self-assembly embedded Dex-AE/PEGDA hydrogel (Figure 1D) were prepared. Similar to the pure PEGDA hydrogel, the pure Dex-AE/PEGDA hydrogel had no signs of aggregates (DBC-0), but the self-assembly embedded hydrogel showed some aggregates (DBC-5). Unlike those aggregates that stuck together in the pure PEGDA hydrogel (Figure 1B), these aggregates were evenly distributed in the hydrogel (Figure 1D).

A comparison indicated that the observed aggregates can be attributed to the self-assembly from Dex-BH and Dex-CA; Dex-AE had an obvious effect on the distribution of the self-assembly. The pure PEGDA hydrogel provided a chemically homogeneous environment for the embedded self-assembly and did not have a strong interaction with the self-assembly; however, when the self-assemblies were charged, they interacted with each other, leading to the aggregation. When Dex-AE was introduced

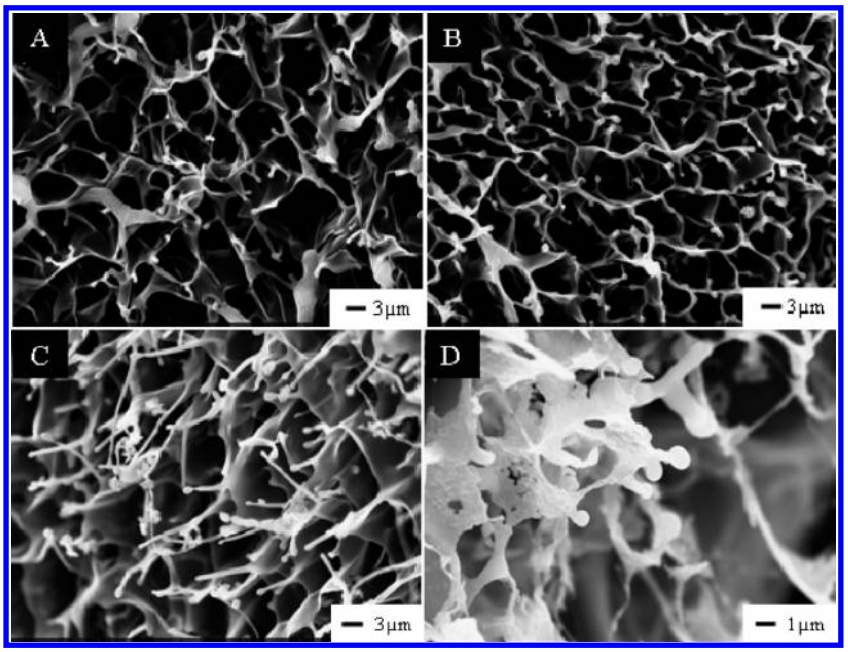

Figure 2. Effect of self-assembly precursor concentration on the SEM micrographs of the tube-embedded hydrogel: (A) DBC-5; (B) DBC-10; (C) DBC-15; (D) DBC-10 after 4 months in PBS (pH7.4).

into the hydrogel, the amine groups protonated and interacted with the self-assembly; i.e., Dex-AE provided binding sites for the self-assembly and directed their growth and distribution. Therefore, the self-assemblies did not aggregate or stick to each other.

Effect of Dex-BH/Dex-CA Feeding Amount on the Self-Assembly Distribution. The change in self-assembly distribution in the hydrogel was evident, suggesting that Dex-AE had a strong interaction with the embedded self-assembly. To further investigate the effect of Dex-AE on the distribution of the self-assembly, different amounts of self-assembly precursors were added to the hydrogels. Figure 2 shows the morphology of the self-assembly embedded hydrogels with different amounts of self-assembly. From hydrogel DBC-5 to hydrogel DBC-15, the increase in the self-assembly precursor feeding amount caused the changes in the size and distribution of self-assembly. In DBC-5 (Figure 2A), few sphere-like self-assemblies dispersed in the hydrogel; their size was approximately 1.22 ± 0.40 μm. In DBC-10 (Figure 2B), there were more sphere- and/or tubule- like self-assemblies present in the hydrogel, and their size was around 1.98 ± 0.46 μm. In DBC-15 (Figure 2C), complete tubular structures formed that were about 9.71 ± 2.84 μm.

Because the hydrogel precursors made no changes from DBC-5 to DBC-15 and the self-assembly had no direct involvement in hydrogel cross-linking, the hydrogel network structures were very similar; therefore, the difference in self-assembly can be attributed solely to their feed compositions. For the self-assembly precursors, at a lower feeding amount (Figure 2A), the hydrogel (Dex-AE) had enough binding sites available for the self-assembly to occupy; thus the self-assembly were evenly distributed and had smaller sizes. As the feeding amount increased, the self-assembly occupied the binding site first, and then started to grow, so there are combinations of sphere-like and tubular structures present in the network (Figure 2B). As the feeding amount continued to increase, the self-assembly occupied all binding sites before growing to larger dimensions (Figure 2C).

It was found that all the self-assemblies are located on the edge of the network and protrude into the pore channels. This protrusion should be attributed to the hydrophilicity of the self-assemblies. As both Dex-BH and Dex-CA are hydrophilic, the newly assembled aggregates are hydrophilic as well, thus they are water-loving, and tend to protrude into water.

Meanwhile, we also examined the stability of the self-assembly. In this study, we observed the morphology of DBC-10 after being immersed in PBS (pH7.4) for 4 months. Figure 2D shows that DBC-10 degraded and lost some network integrity after 4 months, while some self-assemblies are still in good shapes. This indicates that pH4.0 is the only the essential for self-assembly formation, but not necessary for maintaining their structures. Once the self-assemblies are formed, the intermolecular forces are much stronger than ionic forces alone, and these self-assemblies are very stable regardless of pH values.

FTIR Study. The above morphology studies clearly indicate that the distribution of the self-assemblies was strongly influenced by the introduction of Dex-AE to the hydrogel. A FTIR study further confirmed the interactions between the self-assembly and the hydrogel. Figure 3 shows the spectra of Dex-BH, Dex-CA, and their self-assembly as well as the hydrogel and its self-assembly impregnated hydrogel. According to our previous study,[40] the absorption at 1635 cm^{-1} (peak 1) in spectrum A is caused by the N−H bending vibration of amine group, while the band at 1748 cm^{-1} (peak 2) in spectrum B is caused by the C═O stretching vibration of Dex-CA; this confirms the incorporation of amine groups and carboxylic acid groups, respectively. In spectrum C, the absorption at 1675 cm^{-1} (peak 3) and 1563 cm^{-1} (peak 4) can be attributed to the N−H asymmetric bending of NH_3^+ and the C−O asymmetric stretching of the carboxylate anion ($-COO^-$), respectively. This spectrum reveals the presence of protonated amine groups and dissociated carboxylic acid groups, which can interact with each other via electrostatic force to form self-assembling tubules.

Spectrum D is pure Dex-AE/PEGDA hydrogel; the absorptions at 1699 (peak 6) and 1528 cm^{-1} (peak 5) are assigned to amide I and amide II, respectively. However, the implantation of the self-assembly into the hydrogel changed the location of the two peaks, which shifted to 1723 (peak 8) and 1536 cm^{-1} (peak 7) (spectrum E), respectively. The shift to higher frequency was attributed to the hydrogen bonding formation between the

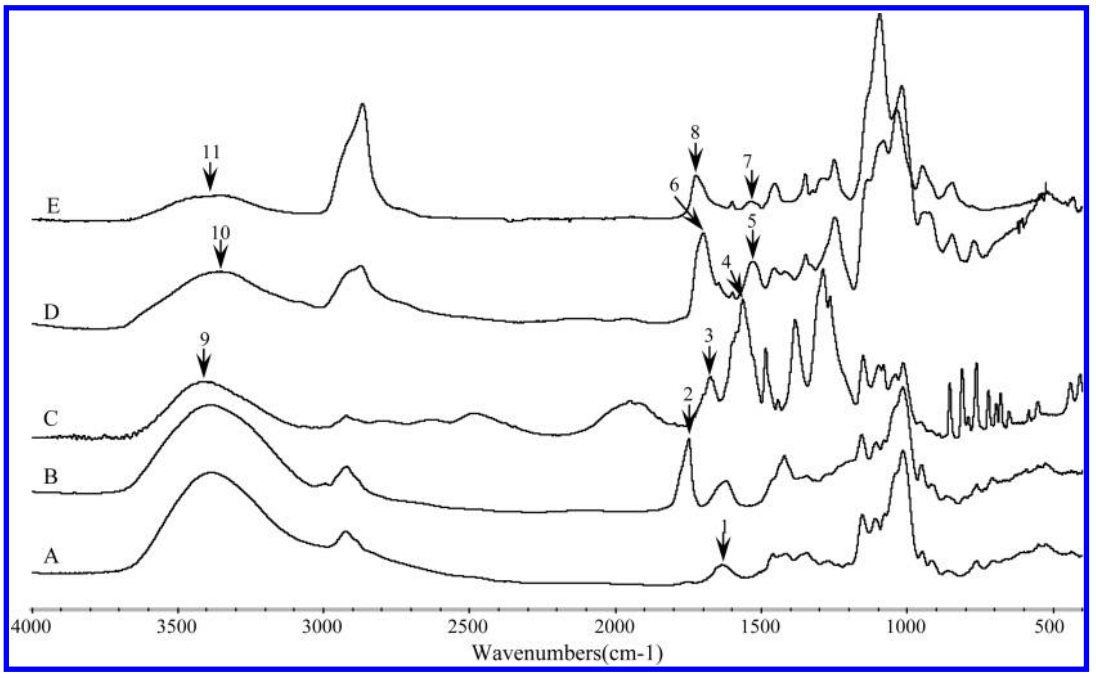

Figure 3. FTIR study of the tube embedded into Dex-AE/PEGDA hydrogel: (A) Dex-BH; (B) Dex-CA; (C) self-assembly; (D) Dex-AE/PEGDA hydrogel; (E) self-assembly embedded hydrogel hybrid. Key: 1, 1635 cm^{-1}; 2, 1748 cm^{-1}; 3, 1675 cm^{-1}; 4, 1563 cm^{-1}; 5, 1528 cm^{-1}; 6, 1699 cm^{-1}; 7, 1536 cm^{-1}; 8, 1723 cm^{-1}; 9, 3420 cm^{-1}; 10, 3348 cm^{-1}; 11, 3362 cm^{-1}.

urethane groups of Dex-AE and the carboxylic and amine groups of the self-assemblies. Furthermore, the self-assembly had a peak at 3420 cm^{-1} (peak 9), and the hydrogel had a peak at 3348 cm^{-1} (peak 10); the peaks shifted medially to 3362 cm^{-1} (peak 11) when the self-assembly implanted into the hydrogel, which indicates the interaction between the self-assembly and amine groups of the hydrogel.

The results revealed by the FTIR demonstrate that self-assembly could form in hydrogel and the amine groups can provide binding sites for self-assembly, which can guide their growth. A schematic illustration for the self-assembly within the hydrogel and their interactions are given in Figure 4.

Effect of Dex-AE Concentration on the Morphology of Self-Assembly. To further confirm the effect of amine groups (Dex-AE) on the growth and distribution of the self-assembly, the effect of Dex-AE concentration on the morphology of self-assembly was examined by doubling the amount of the Dex-AE component in the hydrogel, keeping all other components unchanged. Figure 5 shows the morphologies of hydrogel DBC-15 and hydrogel DBC-15″, in which Dex-AE was doubled. From the SEM micrograph, it is roughly estimated that the self-assembly in DBC-15 (Figure 5A) is about 9.71 ± 2.84 μm, while the self-assembly in DBC-15″ (Figure 5B) is around 2.31 ± 0.81 μm. The self-assembly in hydrogel DBC-15 is obviously longer than the self-assembly in hydrogel DBC-15″. However, the self-assembly in DBC-15″ has a more of even distribution than those in hydrogel DBC-15.

The doubling of the Dex-AE component increased the number of amine groups within the hydrogel. Because the amine groups can provide the binding sites for self-assembly, the hydrogel provides more binding sites for self-assembly when the amount of Dex-AE increases. The self-assembly first occupied those binding sites before growing; as a result, more self-assembles formed when there were more binding sites. However, as those self-assembly components were consumed, there were not enough components available for further self-assembly growth, thus leading to smaller but more evenly distributed self-assembly.

Swelling Study. Figure 6 shows the effect of the amount of self-assembly on the equilibrium swelling ratio of the hydrogels. The data show that an increase in self-assembly component feeding amount led to a slightly reduced swelling. For example, the equilibrium swelling ratio was 970% for the pure Dex-AE/PEGDA hydrogel (DBC-0), while for hydrogel DBC-15, the equilibrium swelling ratio was around 870%, i.e., approximately a 10% decrease.

Because the implantation of self-assembly into the hydrogel did not significantly change the swelling property of the hydrogel, there was no remarkable effect on the hydrogel structures. Our previous studies[2,39] found that the swelling of the Dex-AE/PEGDA hydrogels was mostly dominated by network structures other than their chemical structures. As the size of self-assembly in the hydrogel increased with the increase in self-assembly feeding amount, there was more free room available in DBC-5, but that space was occupied by the newly formed self-assembly in DBC-15. Consequently, the reduced space led to slightly decreased swelling capability.

In Vitro Albumin Release Study. *Loading Efficiency.* As illustrated in Figure 4, the implantation of tubular self-assemblies within the hydrogel includes both self-assemblies and photo-cross-linking; as a result, the OVA should be located in these two carriers as well. Thus, the loaded OVA can be roughly divided into two domains, the self-assembly and the hydrogel, except for pure Dex-AE/PEGDA hydrogel. The OVA loading capacity of pure Dex-AE/PEGDA hydrogel and the self-assembly implanted hybrid hydrogels are shown in Table 2. The OVA loading efficiency for pure Dex-AE/PEGDA hydrogel (DBC-0) is 91.89%, lower than the 94.41%, 96.54% and 93.49% for DBC-5 DBC-10 and DBC-15, respectively. This can be attributed to the implanted self-assemblies, which improved OVA absorption ability.

As indicated by the table, OVA has a similar loading efficiency in self-assembled tubules. DBC-5 (61.59%) and DBC-10 (61.89%) are very close, and a little higher than DBC-15 (56.34%). This could be attributed to the self-assembly dimension

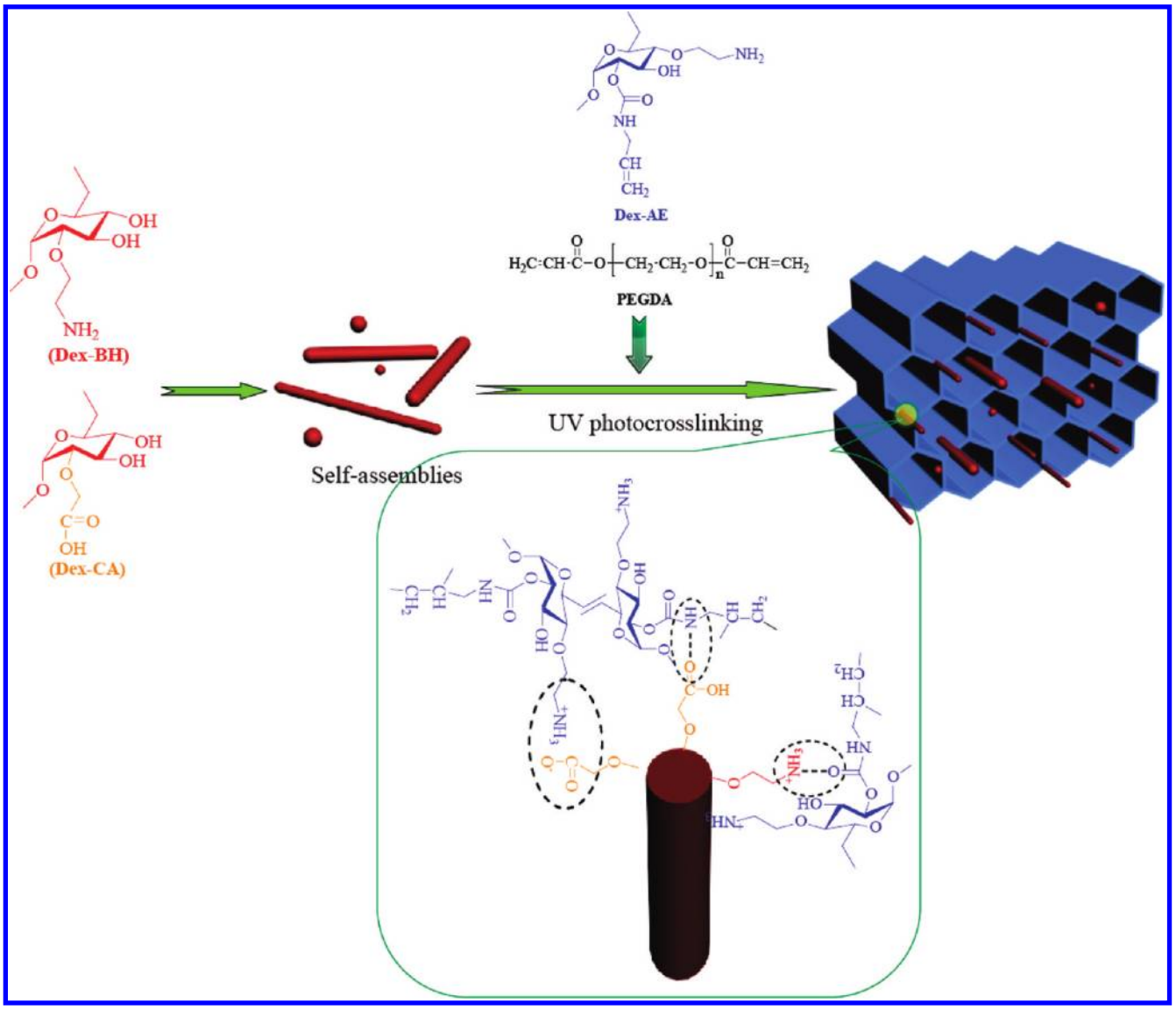

Figure 4. Illustration of self-assembly implantation into hydrogel.

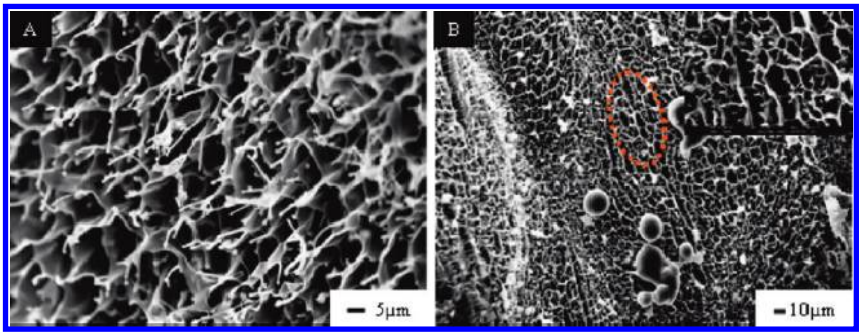

Figure 5. Effect of hydrogel precursor feed ratio on the morphology of the tube-embedded hydrogel: (A) Dex-AE/PEGDA = 3/7; (B) Dex-AE/PEGDA = 6/7. The self-assembly components feeding amounts are the same.

difference. Because OVA is hydrophilic, it is fond of water and tends to locate or disperse to the outer layer of the self-assembly. When the self-assembling tubules become larger, they will have a smaller surface-to-volume ratio, leading to reduced OVA loading capability. Except for DBC-0, the hydrogels entrapped 32.82%, 34.65%, and 37.15% from DBC-5 to DBC-15, respectively. On the basis of the information here, the ratio between the OVA loaded in self-assembly and hydrogels is roughly about 2:1, which indicates that most of the OVA loaded into the self-assemblies.

Cumulative Release. The cumulative OVA release from the Dex-AE/PEGDA hydrogel and the self-assembly implanted Dex-AE/PEGDA hydrogels in pH 7.4 PBS are shown in Figure 7. Figure 7A shows that hydrogel DBC-0 had a higher burst release and faster continuous release than other self-assembly implanted

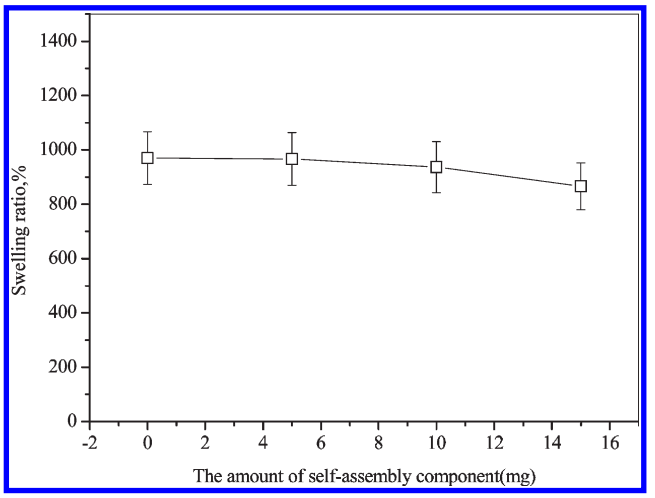

Figure 6. Equilibrium hydrogel swelling ratio as function of the amount of Dex-BH (or Dex-CA).

Table 2. OVA Loading Efficiency into Pure Dex-AE/PEGDA Hydrogel and its Tube-Embedded Hydrogel

	sample ID			
	DBC-0	DBC-5	DBC-10	DBC-15
initial feeding,[a] %	100	100	100	100
actual loading,[b] %	91.89	94.41	96.54	93.49
portion loaded into tubules,[c] %	[d]	61.59	61.89	56.34
portion loaded into hydrogel, %	91.89	32.82	34.65	37.15

[a] The initial loading amount was 6 mg/sample. [b] The actual loading amount was calculated by subtracting the unloaded OVA. [c] The loaded OVA was assumed to be entrapped by either the assembly or the network. [d] No assembly formed.

hydrogels. For example, after 2 days, about 21% OVA released from hydrogel DBC-0, but only 14% OVA released from DBC-5, DBC-10, and DBC-15. The OVA releases from DBC-5 to DBC-15 were very similar, and their release profiles were close during the first 6 days. However, after 6 days, the difference becomes evident. For example, at the end of 50 days, DBC-0 release was 45%, which is still higher than others, while the release from DBC-5, DBC-10 and DBC-15 was 36%, 33%, 30%, respectively.

The release difference between the nonself assembly implanted hydrogel (DBC-0) and the self-assembly implanted hydrogels (DBC-5, -10, -15) is attributed to the introduction of the self-assembly. For OVA loaded in the self-assembly, it will be released first into the hydrogel and then into the media, thus leading to a slower release. According to the loading efficiency study, about 60% of loaded OVA is located within the self-assembly; therefore, the release is slowed by introducing the self-assembly. The release difference between the self-assembly implanted hydrogels can be attributed to the dimension of the self-assembled structures. Because the self-assembly in hydrogel DBC-15 is the largest, the OVA loaded in the self-assembly would take a longer time to be released, so the release time is slower than the others.

To further investigate how the OVA in self-assembles contributed to the above release, we examined the release from pure self-assemblies. Figure 7B shows the release from pure self-assemblies at different loading amount. The data indicate SA10−25 has the fastest release than others, and the release decreases with the OVA loading amount. For example, within 20 days, 61% OVA were released from SA10−25, while 31% and 17% OVA were release from SA10−50 and SA10−100,

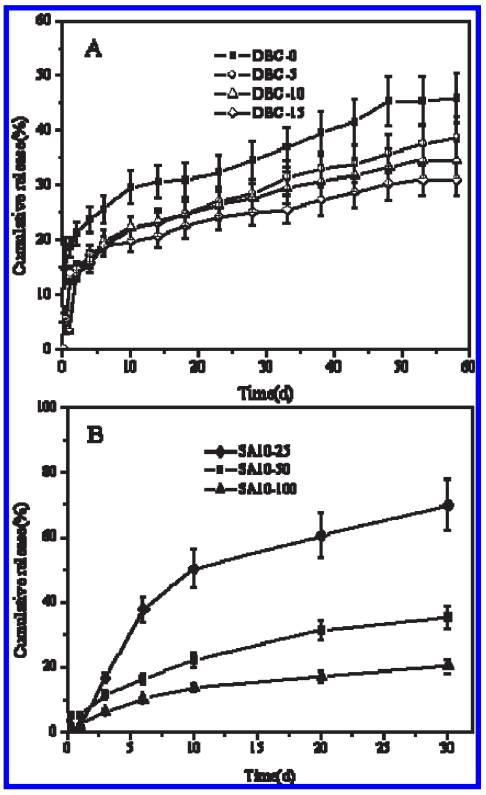

Figure 7. Cumulative release of OVA from (A) tube-embedded hydrogels and (B) self-assemblies at 37 °C and pH 7.4.

respectively. However, based on their original loading amount, the absolute release amount was quite close to each other. This again indicates that OVA tend to locate at the outer layer of the self-assemblies because of the hydrophilic property of OVA, an only those OVA located at outer layer were released. Meanwhile, Figure 2D indicates that the self-assemblies were very stable, which may account for, for example, why only 30% OVA were released from SA10−50 within 30 days.

Conclusion

This study demonstrates that Dex-BH and Dex-CA were self-assembled into tubular structures and successfully embedded into the Dex-AE/PEGDA hydrogels. The morphology study by SEM revealed the interactions between the Dex-AE/PEGDA hydrogel and the self-assembly as well as the hydrogel influence to the growth and distribution of the self-assembly. The interactions between the self-assembly and the hydrogel were confirmed by FTIR data; and further study indicated that self-assembly tends to occupy the binding sites within the hydrogel before they can grow. The swelling test suggested the implantation of self-assembly had no prominent effect on the hydrogel network structures. The drug loading efficiency study showed that more than 60% OVA were located in the self-assembled entities. Moreover, the drug release test revealed that the implantation of self-assembly reduced the burst release and slowed down the release. Meanwhile, these results may suggest that separate encapsulations within both self-assembly and hydrogel could allow this self-assembly impregnated hydrogel to function as a dual drug carrier.

Acknowledgment. We are grateful for the financial support of the College of Human Ecology (assistantship to G. Sun), which made the study possible.